Geoscience Frontiers 12 (2021) 101188

Contents lists available at ScienceDirect

Geoscience Frontiers

journal homepage: www.elsevier.com/locate/gsf

Research Paper

Nanorocks, volatiles and plate tectonics

Gautier Nicoli [a,*], Silvio Ferrero [a,b]

[a] Institut für Geowissenschaften, Universität Potsdam, 14476 Potsdam-Golm, Germany
[b] Museum für Naturkunde (MfN), Leibniz-Institut für Evolutions- und Biodiversitätsforschung, 10115 Berlin, Germany

ARTICLE INFO

Article history:
Received 4 December 2020
Revised 10 February 2021
Accepted 13 March 2021
Available online 3 April 2021
Handling Editor: R.M. Palin

Keywords:
Nanorocks
Plate tectonics
Volatiles
Lower crust

ABSTRACT

The global geological volatile cycle (H, C, N) plays an important role in the long term self-regulation of the Earth system. However, the complex interaction between its deep, solid Earth components (i.e. crust and mantle), Earth's fluid envelopes (i.e. atmosphere and hydrosphere) and plate tectonic processes is a subject of ongoing debate. In this study we want to draw attention to how the presence of primary melt (MI) and fluid (FI) inclusions in high-grade metamorphic minerals could help constrain the crustal component of the volatile cycle. To that end, we review the distribution of MI and FI throughout Earth's history, from ca. 3.0 Ga ago up to the present day. We argue that the lower crust might constitute an important, long-term, volatile storage unit, capable to influence the composition of the surface envelopes through the mean of weathering, crustal thickening, partial melting and crustal assimilation during volcanic activity. Combined with thermodynamic modelling, our compilation indicates that periods of well-established plate tectonic regimes at <0.85 Ga and 1.7–2.1 Ga, might be more prone to the reworking of supracrustal lithologies and the storage of volatiles in the lower crust. Such hypothesis has implication beyond the scope of metamorphic petrology as it potentially links geodynamic mechanisms to habitable surface conditions. MI and FI in metamorphic crustal rocks then represent an invaluable archive to assess and quantify the co-joint evolution of plate tectonics and Earth's external processes.

1. Introduction

The global volatile cycle (e.g. H, C, N), key to the long-term, self-regulation of the Earth system, relies on the continuous redistribution of elements between Earth's fluid envelopes (i.e. atmosphere and hydrosphere) and the its solid layers (i.e. crust and mantle) (Houlton et al., 2018; Lee et al., 2019). Introduction of volatiles into the terrestrial mantle may have triggered plate tectonics, which as best as we know could have been important for the emergence of complex life (Albarede, 2009). In the Phanerozoic, volcanic activity and subduction drive volatile exchanges between the solid Earth and the surface in extensional and convergent settings (e.g. Kelemen and Manning, 2015; Lee et al., 2019; Plank and Manning, 2019; Wong et al., 2019; Werneret al., 2019). This has been used to support the idea that plate tectonics, through the expression of the Wilson cycle (subduction – collision – rifting) might control in turn the long-term volatile cycle (e.g. Wong et al., 2019 and references therein). The stability of the Earth system would then depend on the positive feedback between surface conditions and geodynamic mechanisms (Lenardic et al., 2019; Sobolev and Brown, 2019).

In collisional settings, reworking of the continental crust is the result of the combination of partial melting, deformation and melt segregation processes. The partial melting of buried supracrustal lithologies (e.g. Chappell and Stephens, 1988; Clemens, 1990, 2003; Villaros et al., 2009; Clemens et al., 2011) mobilises a substantial amount of mineral-bound volatiles (e.g. H_2O, CO_2) at deep crustal levels (e.g. Nicoli and Dyck, 2018; Nicoli, 2019). Along the PT path, the formation of anatectic liquids ultimately leads to the formation of S-type granites, after extraction from the source region and migration into the shallow crust (Clemens et al., 2011). The cogenetic links between the source, the migmatites and the resulting granites (e.g. Nicoli et al., 2017; Nicoli and Dyck, 2018; Clemens, 1990), embodies directly the connection between erosion and weathering processes at the surface, responsible for the formation, the volume and the composition of sediments (Condie, 1993), and the metamorphism and melting at depth. The capacity of the surface reservoir signature (i.e. organic N and C isotopic signature) to be retained beyond partial melting conditions in the lower crust indicates that a significant amount of volatiles can be isolated from the surface cycle and stored in

* Corresponding author.
E-mail address: nicoli@uni-potsdam.de (G. Nicoli).

https://doi.org/10.1016/j.gsf.2021.101188

Table 1
List of case studies of primary melt inclusions (both nanorocks and glassy) and/or fluid inclusions in peak minerals from crustal rocks. When fluid presence during melting is inferred, i.e. not directly verified via identification of primary fluid inclusions, this is reported in the "Note" column. The criteria used to compile this dataset are discussed in the text.

Locality	Age (Ma)	±1σ	P (GPa)	±1σ	T (°C)	±1σ	T/P	Rock	Protolith	Host	MI	FI	Fluid	Note on inclusions	Ref.
El Hoyazo - Mazarrón (Spain)	9.6	*0.3*	0.60	*0.1*	850	*50*	1417	Granulitic enclaves	Sediments	Grt/Pl/Crd/Spl	x	x	COH-N		Acosta-Vigil et al. (2007); Cesare et al. (2007); Ferrero et al. (2011)
Seram, eastern Indonesia	16.0		0.80		950		1188	Felsic granulites	Sediments	Garnet	x				Pownall et al. (2019)
Barun Gneiss (Himalayas)	30.0	*8*	0.80		830	*30*	1038	Migmatites	Sediments	Garnet	x				Ferrero et al. (2012)
Gruf granulite	33.0	*4*	0.90	*0.05*	900	*10*	1033	Felsic granulites	Sediments	Garnet	x	x	COHN	C-Dominated inclusion	Gianola et al. (2020)
Kali Gandaki (Himalayas)	38.5	*2.5*	1.05	*0.05*	685	*35*	652	Migmatites	Sediments	Garnet	x				Bartoli et al. (2019); Carosi et al. (2015)
Rhodope Metamorphic Province (Greece)	40.0		1.35	*0.15*	775	*25*	574	Paragneisses	Sediments	Garnet	x			Carbonate in inclusions	Mposkos et al. (2009)
Maghrebian basement (Tunisia)	12.0	2	0.55	*0.15*	780	*20*	1418	Xenocrysts	Granitoids	Garnet	x	x	COH-N		Ferrero et al. (2014)
Altai orogenic belt (China)	255.8	*1.8*	0.45	*0.05*	850	*50*	1889	Mafic granulites	Mafic rocks	Garnet		x	Pure CO_2	C-Dominated inclusion	Li et al. (2004)
Jubrique, Betic Cordillera (Spain)	287.0	*4*	1.30	*0.1*	850		654	Migmatites	Sediments	Garnet	x	x	CO_2-rich		Barich et al. (2014)
Ivrea Zone (NW Italy)	270.0	*30*	0.80		800		1000	Migmatites	Sediments	Garnet	x	x	COH-N		Carvalho et al. (2019)
Altai orogenic belt (China)	284.1	*2.6*	0.80		980		1225	Pelitic granulites	Sediments	Garnet	x				Liu et al. (2020)
Ronda migmatite (Spain)	286.0	*11*	0.48	*0.03*	680	*20*	1432	Migmatites	Sediments	Garnet	x				Bartoli et al. (2014)
Oberpfalz area, SW Bohemian Massif (Central Europe)	325.0	*50*	0.65	*0.15*	800		1100	Migmatites	Sediments	Garnet	x	x	COH-N	Nanocarbonatites	Ferrero et al. (2016a)
Bavarian Unit (Bohemian Massif)	335.0	*5*	0.60		870	*40*	1450	Paragneisses	Sediments	Garnet	x				Ferrero et al. (2018b)
Blansky Lés (Bohemian Massif)	335.0	*5*	2.25	*0.50*	950		422	Felsic granulites	Granitoids	Garnet	x				Ferrero et al. (2018b)
Hartsteinwerk loja quarry (Bohemian Massif)	335.0	*5*	0.75	*0.15*	775	*25*	1033	Paragneisses	Sediments	Garnet	x				Ferrero et al. (2018b); Sorger pers.comm.
Ktis (Bohemian Massif)	335.0	*5*	1.80	*0.4*	800	*100*	889	Paragneisses	Sediments	Garnet	x	x	COH-N		Ferrero et al. (2018b)
Mohsdorf (Bohemian Massif)	335.0	*5*	1.60		1000		625	Felsic granulites	Granitoids	Garnet	x				Ferrero et al. (2018b)
Plaimberg (Bohemian Massif)	335.0	*5*	4.50	*0.50*	1000	*100*	244	UHP eclogites	Mafic rocks	Garnet	x				Ferrero et al. (2018b)
Saidenbach (Bohemian Massif)	335.0	*5*	4.50	*0.50*	1000		222	Felsic granulites	Sediments	Garnet	x			Diamond	Stöckhert et al. (2001)
Steinaweg (Bohemian Massif)	335.0	*5*	1.85	*0.45*	825	*25*	446	Felsic granulites	Granitoids	Garnet	x				Ferrero et al. (2018b)
Stuckestein (Bohemian Massif)	335.0	*5*	0.60	*0.10*	800		1333	Migmatites	Sediments	Garnet	x	x	COH-N		Ferrero et al., (2018b)
T7 borehole (Bohemian Massif)	335.0	*5*	4.50	*0.50*	1000		222	Felsic granulites	Sediments	Garnet	x			Diamond	Kotkova et al. (2014)
Erzgebirge (Bohemian Massif)	340		4.5		1000		222	Eclogites	Basaltic dyke?	Garnet	x			Metasomatic melt	Borghini et al. (in prep)
Granulitgebirge (Germany)	340.0		2.10	*0.10*	1000	*7.5*	480	Eclogites	Gabbro?	Garnet	x			Metasomatic melt	Borghini et al. (2020)
Orlica-Śnieżnik Dome (Bohemian Massif)	340.0	*50*	2.70		875	*12.5*	329	Felsic granulites	Granitoids	Garnet	x				Ferrero et al. (2015)
Central Maine terrane (USA)	379.0		1.80		1050		1000	Felsic granulites	Sediments	Garnet	x				Axler and Ague (2015); Ferrero et al. (2021)
Gory Sowie (Bohemian Massif)	400.0		0.75	*0.10*	950	*50*	1267	Felsic granulites	Granitoids	Garnet	x				Słupski et al. (2018)
Khabarny mafic–ultramafic Massif (Urals)	415.0	*8*	0.80	*0.03*	785	*45*	981	Garnetites	Mafic rocks	Garnet		x	COH-N		Bakker et al. (2020)
Seve Nappe Complex (Scandinavian Caledonides)	455.0	*5*	4.00		835	*5*	209	Paragneisses	Sediments	Garnet	x	x	COH-N	Diamond	Klonowska et al. (2017)
Mont Albert ophiolitic complex	456.0	*5*	1.00		850		850	Metapelites	Sediments	Garnet	x				Dubacq et al. (2019)
MT. Edixon (Antartica)	515.0	*15*	0.80	*0.1*	760	*20*	950	Schists	Sediments	Garnet	x	x	COH-N		Ferri et al. (2020)
Khondalite Belt (Southern India)	525.0	*5*	0.60	*0.10*	900		1500	Migmatites	Sediments	Garnet	x				Ferrero et al. (2012)
Kokchetav Massif (Kazakhstan)	530.0		4.75	*0.25*	975	*25*	205	Paragneisses	Sediments	Garnet	x			H_2O-K fluid	Stepanov et al. (2016)
Dronning Maud Land (Antartica)	542.0	*27*	1.55	*0.15*	910	*50*	587	Mafic granulites	Mafic dikes	Garnet	x				Ferrero et al. (2018b)
Hakurutale granulites (Sri Lanka)	550.0	*50*	0.95	*0.05*	830			Al, Mg-rich granulite	Metabasite?	Garnet		x	CO_2-rich		Bolder-Schrijver et al. (2000)
Lützow-Holm Complex, East Antarctica	550.0	*50*	0.95	*0.25*	875	*75*	921	Mafic granulites	?	Garnet	x				Saitoh and Tsunogae (2015)
Dronning Maud Land (Antarctica)	565.0	*15*	0.69	*0.04*	1080		1565	Anorthosite	Anorthosite	Plagioclase		x	H_2O-	C-Dominated	Kleinefeld and Bakker

Gore Mountain (Adirondacks, US)	1050.0	*50*	1.00		950		1000	Mafic granulites	Gabbro	Garnet	x			H_2O fluxed	(2002)
Hooper Mine (Adirondacks, US)	1100.0	*50*	1.20		950			Mafic granulites	Mafic rocks	Garnet	x				Ferrero et al. (in prep.)
Port Leyden (NY, US)	1145.0	*29*	0.66	*0.06*	850	*20*	1288	Paragneisses	Sediments	Garnet	x				Nicoli unpublished
Nilgiri massif granulites (Southern India)	2500.0		0.95	*0.05*	740	*10*	779	Felsic granulites	Granitoids	Grt, Qz, Pl		x	CO_2-rich	C-Dominated inclusion	Darling (2013)
															Srikantappa et al. (1992)
Shevroy Hills (Indian craton)	2550.0	*150*	1.00	*0.1*	770	*30*	770	Mafic granulites	?	Garnet		x	CO_2-rich	C-Dominated inclusion	Santosh and Tsunogae (2003)
Athabasca granulite terrane (Canada)	2580.0	*30*	1.00	*0.4*	875	*75*	875	Felsic granulites	Sediments	Garnet	x	x	COH-N	type I	Tacchetto et al. (2019)
Pikwitonei granulite (Canada)	2639.0	*2*	0.65	*0.15*	790	*40*	1215	Granulite	Sediments	Garnet		x	CO_2-rich	C-Dominated inclusion	Vry and Brown (1991)
Limpopo belt	2705.0	*5*	1.10	*0.1*	875	*25*	795	Grt-bearing granitoids	Sediments	Garnet	x	x	COH	Carbonate in inclusions	Safonov et al. (2020)
Uttental (Eastern Greenland)	2800.0							?	?	Garnet	x				Nicoli unpublished

the deep continental crust (Santosh and Omori, 2008; Palya et al., 2011), through burial and metamorphism in convergent margin settings (Houlton et al., 2018; Lee et al., 2019). Ronov and Yaroshevsky (1969) argued that metamorphic rocks (gneiss and schists) contain 10^7 GT of carbon and 10^8 GT of water, representing respectively 25% and 40% of the total volume contained in the continental crust. The existence of such a significant amount of carbon stored in crustal metamorphic rocks is also backed up by electrical conductivity studies, which have suggested the presence of mid- to lower crust graphite films, resulting from the percolation of carbon-rich metamorphic fluids (Frost et al., 1989; Frost and Bucher, 1994; Glover, 1996; Huizenga and Touret, 2012).

Although metamorphic degassing in modern/Phanerozoic collisional settings seems to be taken in consideration when estimating global volatile exchanges (e.g. Lee et al., 2019; Stewart et al., 2019), the role played by the continental crust as a long-term volatile reservoir has often been overlooked. The complex interaction between its deep crustal component and the evolution of plate tectonic processes in regulating the composition of the Earth's external envelopes remains a subject of ongoing debate (Touret, 2003; Santosh and Omori, 2008). In modern convergent settings, the exogenic flux of volatiles from the continental crust can be directly determined by monitoring metamorphic outgassing in active orogenic belts (e.g. Becker et al., 2008; Menzies et al., 2016; Tiwari et al., 2016). Inverse phase equilibria modelling can also be used to recover estimates on the outgassing budget of active and eroded metamorphic belt (Groppo et al., 2017; Rolfo et al., 2017; Stewart and Ague, 2018). However, such an approach allows recovery of information preserved on the retrograde metamorphic path, which only involves secondary fluid fluxes. While information on the volatile budget of the continental crust during prograde metamorphism can be retrieved using exploratory forward phase equilibria modelling (e.g. Kerrick and Connolly, 1998; Nicoli and Dyck, 2018; Nicoli, 2019), an accurate quantification requires the investigation of melt and fluid inclusions and carbonate-rich melt inclusions in exhumed high-grade metamorphic minerals (e.g. Bartoli and Cesare, 2020).

In this study, we reviewed the distribution of melt and fluid inclusions in high-grade rocks through Earth's history. We interrogated an extensive database of case studies of crustal rocks containing melt inclusions, fluid inclusions or both melt and fluid inclusions (Table 1). We examined successively the abundance of anatectic melt inclusions and crustal-derived granites in the geological records and the influence of metamorphic conditions and crustal chemistry on the anatectic melt water content and COH (±N) fluid composition through geologic time. By focusing on the volatile content of melt inclusions, we wanted to bring attention to the critical role the evolution of the continental crust might have played in the regulating of the global volatile cycle.

2. Nanorocks and fluid inclusions

Over the last decade, the study of melt and fluid inclusions in deep crustal lithologies has been a major breakthrough for our understanding of crustal differentiation (Bartoli and Cesare, 2020). The landmark study by Cesare et al. (2009; see also Cesare et al., 2015 and references therein) demonstrated that during the partial melting of the lower crust, pristine anatectic melt can be trapped and preserved as inclusions within grains of refractory peritectic minerals (e.g. garnet) in regionally metamorphosed migmatites. Such inclusions are, in the majority of cases, entirely composed of an aggregate of micrometric crystals, although glassy and partially crystallized inclusions may also be present (Ferrero et al., 2012; Cesare et al., 2015) (Fig. 1a). The mineral phases identified in crystallized melt inclusions are quartz and feldspars (or their poly-

morphs, Ferrero and Angel, 2018) along with OH-bearing minerals and, in few cases, limited amounts of CO_2 and H_2O in interstitial position (Bartoli et al., 2013) (Fig. 1b). Consistently with these observations, such inclusions were originally named *nanogranites* (Cesare et al., 2009) and later *nanogranitoids* (Bartoli et al., 2016). Recent works however showed that crystallized melt inclusions in metamorphic rocks have a much larger variety in composition, i.e. from silicic to carbonatic, prompting Bartoli and Cesare (2020) to spearhead the use of the term "nanorock" as a more comprehensive and appropriate name, and, for this reason, this term will be used throughout the present work. Later studies (Carvalho et al., 2020; Ferrero et al., 2018a; Ferri et al., 2020) have then demonstrated that, besides the anatectic melt, also the fluids present during partial melting can be trapped as primary inclusions in migmatites (Fig. 1c). These fluids consist of CO_2, CH_4, N_2 and H_2O in variable proportions (e.g. Carvalho et al., 2020; Ferrero et al., 2018b; Tacchetto et al., 2019) (Fig. 1d).

Importantly, melt inclusions in metamorphic garnet do not suffer issues commonly recognised in magmatic melt inclusions, such as volatile loss and doubtful correspondence between trapped and original melt due to compositional heterogeneities present in the melt immediately adjacent the growing crystal (i.e. boundary layer effect – see discussion in Cesare et al., 2015). In particular, while diffusive H_2O and CO_2 loss is common for magmatic melt in olivine (Gaetani et al., 2012), driven by the pressure gradient between trapped melt and surrounding magma under continuous depressurisation during ascent, such a driving force is absent in rock-dominated system (i.e. metamorphic rocks during cooling – Bartoli et al., 2014). The H_2O and CO_2 content measured in crack-free melt inclusions in metamorphic garnets can be thus considered as representative of the original volatile content of the melt at depth (more details on the topic in Bartoli et al., 2014; Cesare et al., 2015; Ferrero and Angel, 2018). Boundary layer effects only affect trace elements highly enriched in garnet (e.g. Y, HREE, Acosta-Vigil et al., 2012), thus making the anatectic inclusions overall representative of the original melt composition.

A growing body of evidence (e.g. Carvalho et al., 2020; Ferrero et al., 2016a; Tacchetto et al., 2019 and references therein) has revealed a significant variation in the nature, abundance and distribution of fluid-bearing inclusions in metamorphic minerals. Such variations can be interpreted as resulting from differences in the chemistry of the source, fluid percolation prior entrapment, as well as specific geodynamic settings, which will influence the dehydration/decarbonation sequences along the metamorphic prograde path (e.g. Nicoli and Dyck, 2018; Stewart and Ague, 2018; Stewart et al., 2019 – see section 4 below). The quantification of immiscible pristine COH(±N) fluid phases in rehomogenised nanorocks using NanoSIMS (e.g. Bartoli et al., 2014; Carvalho et al., 2020; Ferri et al., 2020; Ferrero et al., 2021) together with thermodynamic modelling is increasingly becoming a reliable approach to quantify reaction kinetic and thermodynamic equilibrium in the deep continental crust. Importantly, all these applications reassessed the critical role played by fluid-assisted partial melting in accretionary settings, previously relatively neglected – apart from a few remarkable exceptions (e.g. Sawyer, 2010; Weinberg and Hasalová, 2015).

3. Inclusions in space and time

In the present work we employed a database (Table 1) of 46 localities where primary melt (MI) and/or fluid inclusions (FI) have been reported in minerals formed during prograde and peak regional metamorphism of crustal rocks. Out of the whole database, thirty case studies contain only MI, six case studies only FI and ten cases a combination of both trapped at the same time (i.e., under primary fluid-melt immiscibility conditions; see Cesare et al., 2015). The term "MI" refers to polycrystalline inclusions originally trapped as a melt (regardless of their composition, i.e. either silicate rich or carbonatitic), partially crystallized inclusions as well as glassy inclusions. For the purpose of our study, such inclusions are to be considered informative of fluid/melt regime at depth because of their primary nature, i.e. they formed during the growth of the host phase (Roedder, 1984), as well as of the absence of evidence for decrepitation. Fluid inclusions present a different caveat: as thoroughly discussed by Carvalho et al. (2020), most (all?) of the COH(±N) fluid inclusions found in garnet underwent post entrapment changes on cooling with crystallization of new phases. Although this largely prevents a precise quantification of the original fluid composition, their characterisation provides nevertheless precious data on fluid speciation at depth.

Geographically, these findings span all continents with the exception of South America and Australia, and the inferred protolith of the host rocks cover the whole range of rocks, from sediments to granitoid to mafic rocks, involved in continent–continent collision. The most common host for inclusions is peritectic garnet, which is hardly surprising in view of its abundance in metamorphic rocks of crustal origin and its vast range of stability and refractory nature. In some cases, peritectic plagioclase (Madlakana and Stevens, 2018; Nicoli et al., 2017) may also be an important host of inclusions (three case studies). Both peritectic garnet and peritectic plagioclase form in the presence of melt and are cogenetic with MI. The inspection of the database of MI in metamorphic rocks reported by Cesare et al. (2015) shows that zircon is the second most common inclusion host in crustal rocks. However, findings of MI in zircons are left out of the present compilation: zircon crystallizes more often on cooling during the retrograde evolution of the rocks (Roberts and Finger, 1997), and in absence of detailed studies on each case, it is impossible to relate with certainty MI in zircons to the prograde/peak history of the host rocks.

The inclusions discussed here sampled portions of melt and/or fluids present in the deep crust between ~680 °C (Ronda migmatites) and 1050 °C (Central Maine Terrane felsic granulites), and 0.45 GPa (Altai orogenic Belt) to 4.75 GPa (subduction of the continental crust in Kokchetav Massif). Most observations occur at 750–900 °C and ~0.5–1.5 GPa, which correspond to the stability field of granulitic rocks (Harley, 1989) (Fig. 2a). The limited number of findings of MI and FI in ultrahigh pressure (UHP) and ultrahigh temperature (UHT) crustal rocks may be simply related to the relative rarity of such rock types, whereas their absence in high-grade - low pressure crustal rocks is likely due to the absence of peritectic garnet, the most common and reliable host of melt/fluid inclusions, often replaced by the much less robust cordierite. Whereas no particular correlation is visible between different groups and particular PT conditions and/or PT gradients, evidence for the coexistence of crustal melt and a fluid are concentrated in the temperature range 780–900 °C. The fluid is mainly COH(±N) in composition, with a high CO_2 component in most cases (e.g. Carvalho et al., 2019; Cesare et al., 2007; Ferrero et al., 2014, 2018a; Gianola et al., 2020), only two cases showing a H_2O-bearing fluids (Ferrero et al., 2011; Ferri et al., 2020).

For the purpose of this study, the assessment of the role of continental crust evolution in the stabilisation for the global volatile cycle, the most crucial aspect of these findings is their distribution in time (Fig. 2b). The list of case studies covers most of the Earth's history, from 2.8 Ga (Uttental, Greenland) to 9.6 Ma (El Hoyazo, Southern Spain). Most of these inclusions are found in metasedimentary lithologies and few in granitoids and mafic rocks (Fig. 1b). Nanorocks and primary COH(±N) fluid inclusions are mainly a Phanerozoic affair (Fig. 1b). A second cluster of inclusions occurs between 2.5 Ga and 3.0 Ga. These two main periods also correspond to the formation of economically viable graphite

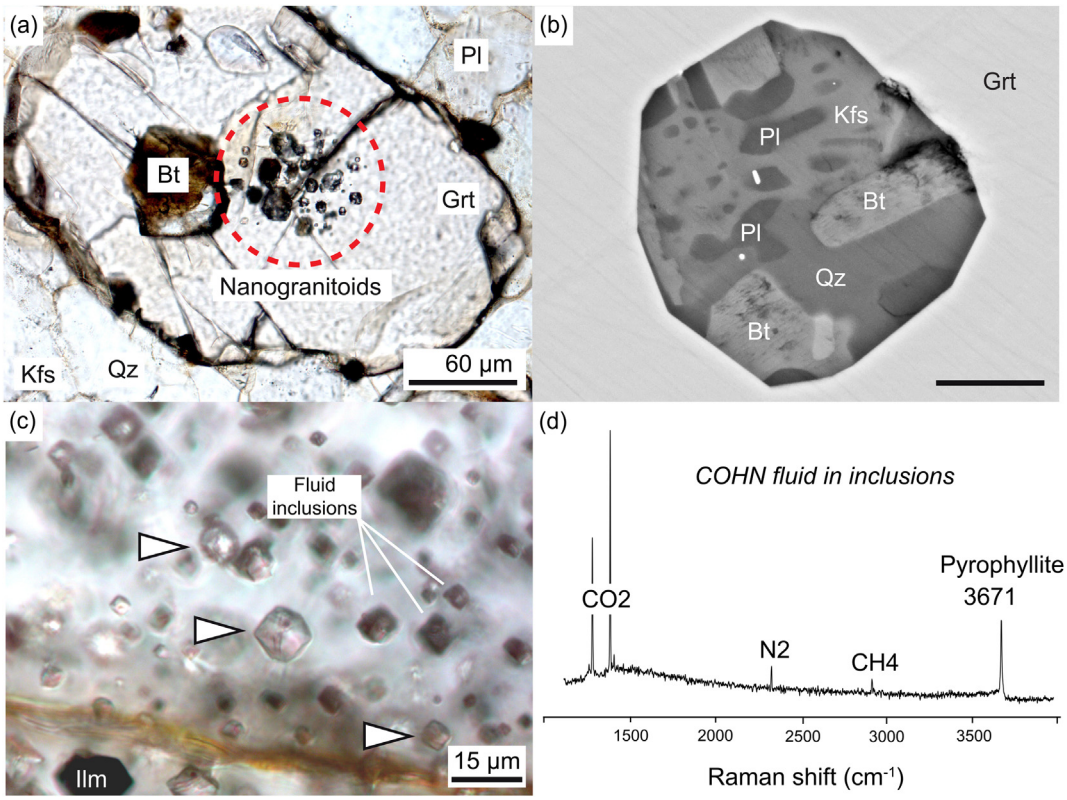

Fig. 1. Nanorocks and fluid inclusions in metamorphic crustal rocks. (a) Typical appearance of a cluster of nanogranitoids in garnet (Ferrero et al., 2016b). Kfs = K-feldspar, Qz = Quartz, Grt = garnet, Pl = plagioclase, Bt = biotite. (b) Nanogranitoid from Koliakkode quarry, Kerala Khondalite Belt (Southern India; PhD thesis S. Ferrero). (c) Nanogranitoids (white arrows) and fluid inclusions in metasediments trapped under conditions of primary fluid-melt immiscibility. Ilm = ilmenite. (d) Typical Raman spectrum of fluid inclusions coexistent with nanogranitoids (Carvalho et al., 2020). Both (c) and (d) are modified after Ferrero et al. (2016a).

deposits (Luque et al., 2014), arguing for major carbon-bearing fluid fluxes in the lower crust (Touret et al., 2016). S-type granites (e.g. Clemens et al., 2011; Zhu et al., 2020) show the same distribution pattern as sediment related inclusions, with a third important peak during the assembly of the Columbia-Nuna supercontinent (1.7–2.1 Ga) (Fig. 2c). Whereas there is evidence of intrusions during the Boring Billion (0.85–1.7 Ga) (Roberts, 2013), only one inclusion in metasedimentary rocks has been identified within this period so far. The issue of preservation bias is mentioned in the discussion below.

The widespread occurrence of inclusion findings across a large range of PT conditions, different protoliths and ages show the capability of natural rocks to sample and preserve deep crustal fluids, making these inclusions reliable probes to investigate planetary scale processes such as fluid regime variations in relationship with plate tectonics. The joint occurrence of nanorocks in metasedimentary rocks, graphite deposits and crustal derived magmas at specific time of Earth's history (Fig. 2b,c) suggests that there might be periods prone to enhanced coupling between crustal reworking and surface mechanisms.

4. Protolith chemistry and partial melting conditions

Nanorocks represent melts and fluids in equilibrium with the bulk rock residue (Acosta-Vigil et al., 2017). The composition of primary melt and fluid phases depends on the chemistry of the source material (e.g. Le Breton and Thompson, 1988; Clemens and Stevens, 2012). In the continental crust, minor compositional variations (e.g. Fe + Mg and K contents) (Condie, 1993) in the upper crust can lead to significant variations in the depth and sequence of devolatilisation events and influence the nature of partial melting reactions and the chemistry of the resulting magmas. For instance, changes in the composition of siliciclastic and volcanoclastic sediments from the Archean to the Phanerozoic are reflected in the evolution of anatectic liquid chemistry towards an increasingly Mg-poor, Ca-rich, less viscous monzogranitic melt (Nicoli and Dyck, 2018; Nicoli, 2019). Although data on the volatile content of primary melt inclusions is still scarce, we compared H_2O and CO_2 contents of rehomogenised inclusions with proposed protolith compositions (Fig. 3a). Protolith with high Ca/(Ca + Na) and Mg# (Mg# = $Mg^{2+}/(Mg^{2+} + Fe^{2+})$) and low-K tend to favour anatectic melt with higher H_2O and CO_2 contents. This is consistent with previous findings (Nicoli and Dyck, 2018; Nicoli, 2019) which have showed that the ferromagnesium content of siliciclastic rocks influences the temperature of mica breakdown and the amount of water available at solidus conditions. Calc-silicate, metacarbonate, and high-Ca siliciclastic rocks are able to retain greatest quantities of carbon under metamorphic conditions typical of accretionary and collision orogenies. This is because most of the metamorphic carbon is held in the crystal structure of the carbonate minerals, calcite [$CaCO_3$] and dolomite [$CaMg(CO_3)_2$], and the stability of these minerals is greatest in compositions high in CaO, SiO_2, and MgO. The composition of primary melt and fluid phases is also determined by where and when along the prograde path they are produced and then entrapped into growing peritectic phases, which then relates to the degree of partial melting. At the mineral scale, the composition is influenced by the interplay between kinetics of diffusion between melt and minerals, the possibility of mineral recrystallization and the time gap between the onset of partial melting and entrapment (Acosta-Vigil et al., 2017). Therefore, the nanorock archive and associated fluid phases in metasedimentary rocks have been primarily used to investigate

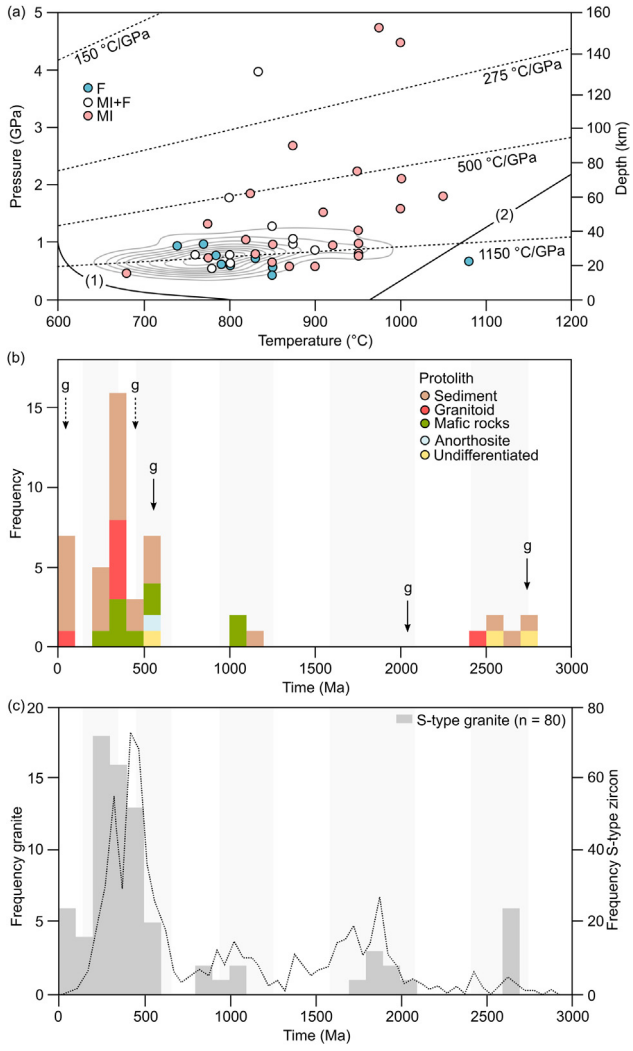

Fig. 2. Nanorocks and primary COH(±N) fluid inclusions. (a) Metamorphic conditions at which melt and fluid inclusions are entrapped by growing peritectic mineral phases (e.g. garnet, plagioclase). 1 - wet granite solidus; 2 – dry granite solidus. The kernel density represents the domain of equilibration of granulitic rocks, from 3.0 Ga to the present (Harley, 1989). (b) Main occurrence of inclusions in high-grade metamorphic mineral in different protoliths. Arrows represent principal graphite deposits (Luque et al., 2014). Dashed line: igneous deposit; plain line: metamorphic deposit. (c) Occurrence of S-type granites (updated database from Clemens et al., 2011; Taylor et al., 2014). The dashed line indicates the occurrence of S-type zircons reconstructed from river sediments (Zhu et al., 2020). Vertical shaded areas represent supercontinent assembly phases.

the primary composition of anatectic melts (e.g. Cesare et al., 2011, 2015; Bartoli et al., 2014), the nature of the melting and reaction and fluid budget of the continental crust (e.g. Acosta-Vigil et al., 2010; Carvalho et al., 2019; Ferrero et al., 2011, 2014, 2016a; Ferri et al., 2020; Gianola et al., 2020; Tacchetto et al., 2019; Acosta-Vigilet al., 2007).

To investigate further the relation between the H_2O and CO_2 content of nanorocks and secular changes in the composition and the thermal state of the crust, we used phase equilibria modelling on average shale bulk compositions from the Archean (2.5–3.0 Ga), Proterozoic (0.6–2.5 Ga) and Phanerozoic (0–0.6 Ga) (Condie, 1993). Shales, primary source of anatectic melts, form from the accumulation of products of weathered continental material in passive continental margins, later remobilised during continental collision (Condie, 1993; Bradley, 2008). We then defined a set of PT paths by considering minimum and maximum orogenic metamorphic gradient (i.e. T/P > 500 °C·GPa^{-1}) over periods of 200 Ma (Brown and Johnson, 2018). We used version 6.9.0 of the Perple_X software package (Connolly, 2009) and the 2004 update of the Holland and Powell (2011) thermodynamic database (http://www.perplex.ethz.ch/) in the system Na_2O-CaO-K_2O-FeO-MgO-Al_2O_3-SiO_2-H_2O-TiO_2 (NCKFMASHT). The solution models used are as follows: silicate melt model, garnet, chlorite, muscovite, biotite, orthopyroxene after White et al. (2014); feldspar (Fuhrman and Lindsley, 1988); amphibole model after Diener and Powell (2012). First, we followed the same approach used by Nicoli and Dyck (2018) and individually fixed bulk-rock water content at the point at which the relevant geotherm intersects the solidus to permit water-absent partial melting. Results are presented in Table 2 and Fig. 3b.

Nanorocks contain a variable amount of H_2O, from 2 wt.% to 14 wt.% (Bartoli et al., 2014, 2019; Carvalho et al., 2019; Ferri et al., 2020) (Fig. 3a). Our modelling reproduces the entire range of observed H_2O contents in anatectic inclusions. The secular evolution of the thermal state of the crust (i.e. apparent metamorphic gradient, T/P - Brown and Johnson, 2018), combined with changes in the shale chemistry (Condie, 1993) directly influences the water content of the melt (Nicoli and Dyck, 2018). Our modelling shows that maximum water contents in the melt is reached for low T/P (<1000 °C·GPa^{-1}) gradient at 0–1.2 Ga, 1.8–2.0 Ga and 2.4–2.8 Ga, corresponding to periods of well-established plate tectonic mechanisms, generalisation of mobile lid tectonics and transition from stagnant lid to mobile lid tectonics respectively (e.g. Condie, 2018; Holder et al., 2019; Palin et al, 2020) (Fig. 3b). Minimum melt water contents are reached during the tectomagmatic lull at 2.2–2.3 Ga (Spencer et al., 2018) and the *Boring Billion*, during which single lid tectonic regimes might have been the dominant geodynamic regimedominated (Stern, 2020). Our modelling also suggests that the range of melt water content for high T/P (>1000 °C·GPa^{-1}) might have been constant since the Archean.

In order to estimate the concentration of CO_2 in the combined melt and the fluid phase, we used the Phanerozoic shale composition in the NCKFMASHT-CO_2, adding a fluid phase (Connolly and Trommsdorff, 1991) and carbonates (Holland and Powell, 2011; Kuhn, 2004) to the solution model. We calculated X_{CO2} (X_{CO2} = CO_2/(CO_2 + H_2O)) between 750 °C and 1150 °C along the two metamorphic gradients encompassing the conditions of rehomogenisations, 650 °C·GPa^{-1} and 850 °C·GPa^{-1}, at fixed bulk H_2O content, 1.75 wt.% and 1.35 wt.% respectively (Table 1) (Fig. 3c). The CO_2 content of nanorocks varies between 180 ppm and 8100 ppm (e.g. Carvalho et al., 2019; Ferri et al., 2020; Gianola et al., 2020; Ferrero et al., 2021). Although the data set is restrained to the Phanerozoic and Neoproterozoic, it is worth noting that there is an apparent positive correlation between concentration in CO_2 in the melt and the temperature (Fig. 3c). The modelling reproduces inclusions with CO_2 concentration <3000 ppm for a maximum X_{CO2} of 0.02. Higher CO_2 concentration values are reached for X_{CO2} between 0.05 and 0.1. It is worth noting that our modelling only considers a single source (i.e. shale). In reality, sediments in passive margins range from quartzite to volcanoclastic to carbonate (Veizer and Mackenzie, 2004). Hence, our modelling only provides an overview of the melting/volatile relationship in the deep continental crust.

5. Discussion

5.1. Connecting nanorocks to the global volatile cycle

The presence of CO_2 in the lower crust has been long argued to be the results of slab decarbonation and fluid flux from the mantle wedge since the late Archean (Newton et al., 1980; Newton, 1987; Santosh and Omori, 2008; Touret et al., 2016). Although ascending CO_2 percolation might still have occurred at the crust/mantle inter-

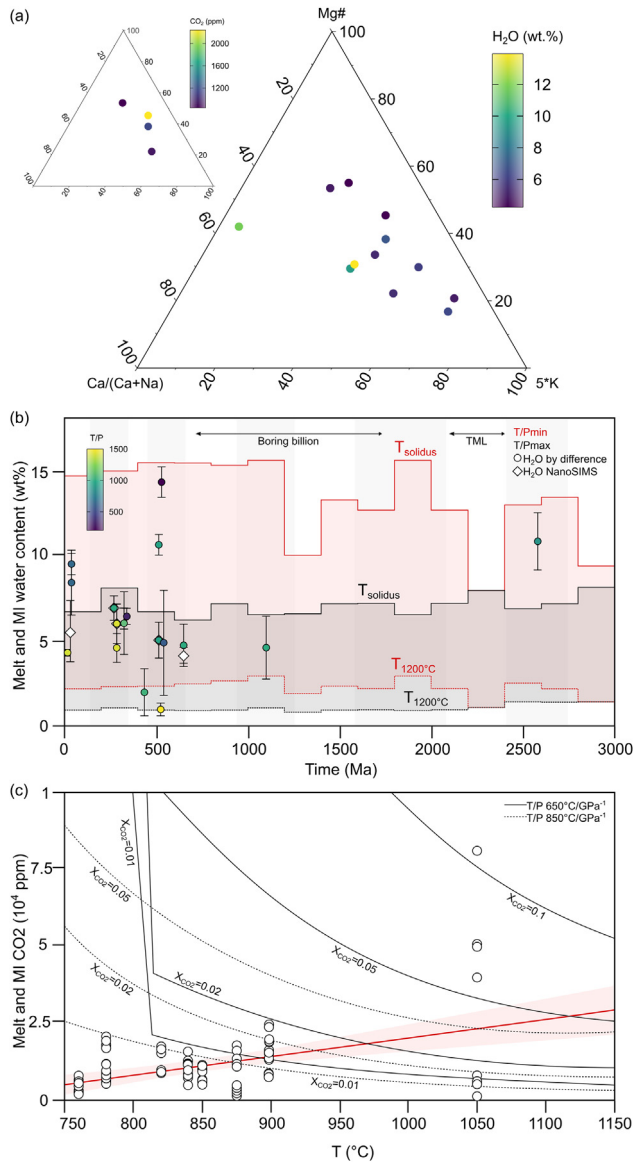

Fig. 3. Water and carbon dioxide content in rehomogenised melt inclusions from metasedimentary rocks estimated by difference from EMP totals or via NanoSIMS analyses. (a) H_2O and CO_2 content in inclusion plotted as a function of bulk rock protolith in Ca/(Ca + Na) – K – Mg# space. Mg# = $Mg^{2+}/(Mg^{2+} + Fe^{2+})$. Both ternary diagrams have identical axes. (b) H_2O content in modelled melt and melt inclusions (MI). The shaded areas represent the range of water content between $T_{solidus}$ and T_{1200} for the minimum and maximum metamorphic gradients for each bin of 200 Ma. Vertical bars areas represent supercontinent assembly. TML: tectomagmatic lull (Spencer et al., 2018). The colour code for each datapoint correspond to the apparent metamorphic gradient (T/P). (c) CO_2 content in modelled melt and melt inclusions (MI) for different X_{CO2} (i.e. $CO_2/(H_2O + CO_2)$) as a function of rehomogenisation temperatures. Linear regression on the average CO_2 content at given temperature with a 1σ error envelope (grey area) is also shown.

face, the primary nature of the nanorocks and associated primary COH(±N) fluids argues in favour of an internally derived source, making these inclusions preserved snapshots of deep crustal reworking processes. Therefore, their presence in metasedimentary rocks has a great potential as it offers a new tool to understand and quantify the transfer of volatile elements from the surface (e.g. formation of the protolith via weathering and erosion) to the lower crust.

In this part of the discussion, we show that the occurrence of MI and FI in high-grade rocks might be linked to the different phases of the Wilson cycle during the Phanerozoic, which as best as we know controls the modern carbon cycle (Wong et al., 2019).

During continental break-up phases (50–150 Ma, 400–500 Ma; Condie et al., 2015), atmospheric CO_2 increased mainly as the results of crustal extension and degassing from rift zones (Berner and Kothavala, 2001; Foley and Fischer, 2017; Wong et al., 2019) (Fig. 4a). During continental assembly phases (150–400 Ma and >500 Ma), the increase in orogenic activity was followed by an increase in the weathering rate (François et al., 1993), drawing CO_2 from the atmosphere into siliciclastic sediments (Berner and Kothavala, 2001) (Fig. 4a). Continental silicate weathering is estimated to currently consume 38–75 MT C·yr^{-1} (e.g., Gaillardet et al., 1999 and references therein). Carbon-bearing sediment amalgamate in passive margins, which are in turn remobilised during continental collision (Bradley, 2008). The burial of supracrustal rocks could then bring a substantial amount of CO_2 and H_2O towards crustal reworking sites. Along the way, devolatilisation reactions releases COH(±N) fluids into the middle crust. Steward et al. (2019) estimated that 2–23 MT C·yr^{-1} are currently produced by metamorphic degassing in collision settings. If we consider these current outgassing rates and that up to half of the weathered continental silicate material deposited in passive margin is ultimately remobilised during crustal thickening, up to 50% of the carbon remains trapped in the root of orogenic belts and preserved passed partial melting conditions.

The occurrence of MI and FI in the geological record coincides with episodes of crustal thickening and high melt productivity (>50 vol%, Fig. 4b). These different observations highlight a ~ 320 Ma cyclicity for the transfer of volatiles from the crustal reservoir to the surface reservoir (Fig. 4b). This is in agreement with the tempo of orogenic activity (~80 Ma) (Brown et al., 2020), the 300 Ma periodicity of the magmatic/volcanic cycle (Brink, 2019) and the fact that the global flux of weathered material recycled into the mantle is currently balanced by addition of material at Earth's surface mainly in accretionary and collisional zones (Scholl and von Huene, 2007; Clift et al., 2009; Hawkesworth et al., 2010; Guo and Korenaga, 2020). Therefore, even if additional mechanisms need to be taken into consideration, such as glaciation (Foster et al., 2017) and cosmic cycles (Berger, 2013; Brink, 2019) (Fig. 4b), orogenic activity (weathering + metamorphism) might be capable to influence Earth's climate every ~160 Ma (Fig. 4b).

The continental crust is the third most important carbon reservoir on Earth (6.5×10^7 GT C), after the core (4×10^9 GT C) and the mantle (3×10^8 GT C) (DePaolo, 2015). Garnet was proposed to represent 4.9 vol% of the total crustal mass (Ronov and Yaroshevsky, 1969), and it is known to form mostly in the T range > 400 °C to > 1000 °C in metamorphosed crustal rocks (Baxter et al., 2013). As melt is stable from T > 700 °C, we considered that ~ 50% of the garnet forms in suprasolidus conditions (i.e. 2.5% of the total crustal mass). Assuming that 30%–50% of the crystal volume of these garnets is occupied by inclusions containing 2–14 wt.% H_2O and 180 ppm and 8100 ppm CO_2 (Parisatto et al., 2018), the current maximum global amounts of water and carbon trapped in nanorocks are 10^5–10^6 GT and 10^3–10^5 GT respectively. As a comparison, these estimates would correspond to the equivalent of one Greenland ice sheet (2.3×10^6 GT H_2O) and one to two Earth's atmosphere (5.9×10^2 GT C) (Eakins and Sharman, 2010; Lee et al., 2019). These estimates are made assuming that all peritectic garnets have inclusions and all inclusions are preserved melt. Therefore, our mass balance calculation only gives an insight into the importance of the formation and stabilisation of a partially molten lower crust on the long-term storage of volatiles in the deep Earth (Touret, 2003). The presence of exposed late Archean metasedimentary granulitic rocks in the geological record (Harley, 1989) would then suggest the duration of this storage could easily exceed 2.5 Ga.

Table 2
Modelled bulk and melt water content along minimum (T/Pmin) and maximum (T/Pmax) orogenic metamorphic geothermal (T/P – Brown and Johnson, 2018) per bin of 200 Ma, using shale compositions from Condie (1993) as starting material.

Bin (Ma)	T/P_{min}					T/P_{max}				
	T/P (°C·GPa^{-1})	$T_{solidus}$ (°C)	H_2O_{bulk} $T_{solidus}$ (wt.%)	H_2O_{melt} T_{1200} (wt.%)	H_2O melt $T_{solidus}$ (wt.%)	T/P (°C·GPa^{-1})	$T_{solidus}$ (°C)	H_2O_{bulk} $T_{solidus}$ (wt.%)	H_2O_{melt} T_{1200} (wt.%)	H_2O_{melt} $T_{solidus}$ (wt.%)
0–200	547	722	1.75	2.14	14.49	1500	722	0.88	0.91	6.71
200–400	518	722	1.75	2.24	14.92	1321	722	0.95	0.98	8.02
400–600	500	722	1.75	2.34	15.38	1500	722	0.88	0.91	6.71
600–800	507	722	1.75	2.34	15.38	1727	722	0.83	0.86	6.19
800–1000	571	722	1.7	2.60	15.18	1517	722	0.93	0.98	7.21
1000–1200	503	722	1.7	2.86	15.53	1629	722	0.93	0.98	6.53
1200–1400	850	735	1.53	1.82	9.91	2111	722	0.8	0.85	6.53
1400–1600	618	735	1.7	2.32	13.31	1500	722	0.93	0.98	7.21
1600–1800	682	735	1.7	2.25	12.61	1493	722	0.93	0.98	7.21
1800–2000	500	722	1.7	2.86	15.53	2000	722	0.8	0.85	6.53
2000–2200	650	735	1.7	2.25	12.61	1600	722	0.93	0.98	7.21
2200–2400	1269	722	0.93	1.00	7.92	1282	722	0.93	1.00	7.92
2400–2600	512	771	1.33	2.59	12.92	1313	735	1.45	1.52	6.92
2600–2800	621	735	1.36	2.25	13.31	1686	710	1.4	1.46	7.12
2800–3000	732	771	1	1.49	9.27	1068	735	1.33	1.49	8.17

Recent publications (Mason et al., 2017; Salem et al., 2019) have demonstrated that in convergent margins, sedimentary carbonates significantly contribute to the carbon budget of active arc volcanoes. About 75% of the emitted carbon would derive from crustal carbonate (Mason et al., 2017). The assimilation of carbon from crustal fluids and metasedimentary rocks has also been observed in continental large igneous provinces (Black and Gibson, 2019). The compilation of melt inclusions and gas emissions data from various tectonic settings highlights the importance of the presence of a crustal reservoir on the exogenic volatile flux budget (Fig. 5). Despite possible degassing effects during magma ascent, melt inclusions in komatiite – proxy for the primitive mantle (Sobolev et al., 2016), and melt inclusion in high-grade metamorphic rocks define two distinct endmembers (Fig. 5a). The primitive mantle, and to some extent mid-oceanic ridge basalts (MORBs), have a low water and low carbon content, unlike anatectic melts (Fig. 5a). The volatile content of plume, rift and arc volcanoes melt can then be interpreted as the results of mixing between the crust and the mantle. The same pattern is found when analysing the isotopic composition (He, C) of gas emission from active volcanoes and shear zones (Fig. 5b). Arc and rift settings display a mixed signature of both a mantle source and a low-metamorphic grade siliciclastic/carbonate source (e.g. Mason et al., 2017). Shear zone and faults might remobilise a significant amount of both high-grade crustal material and organic matter ($\delta^{13}C < -20$) during earthquakes. Thus, the presence of a metamorphic continental reservoir seems to have a long lasting effect on the global carbon cycle. Such fundamental question then links the evolution of Earth's fluid envelopes to the evolution of the crust, plate tectonics and the supercontinent cycle (Touret et al., 2016).

5.2. Implications for the evolution of plate tectonics

In this part, we discuss how the occurrence of nanorocks can help decipher the nature and evolution of geodynamic processes through time. The relative absence, up to date, of studies reporting nanorocks and COH(±N) fluid inclusions in terrains older than 0.6 Ga may be due either to (i) the preferential preservation of the continental crust, or (ii) a preservation issue (i.e. the inclusions originally present in the rock were then erased via as result of extensive rock re-equilibration and deformation) or (iii) a simple lack of data for this period. The first scenario is still disputed. Using the geochronological record, some studies have suggested that peaks in zircon abundance reflect an increase in continental growth rates (e.g. Condie, 1998; O'Neill et al., 2007). In contrast,

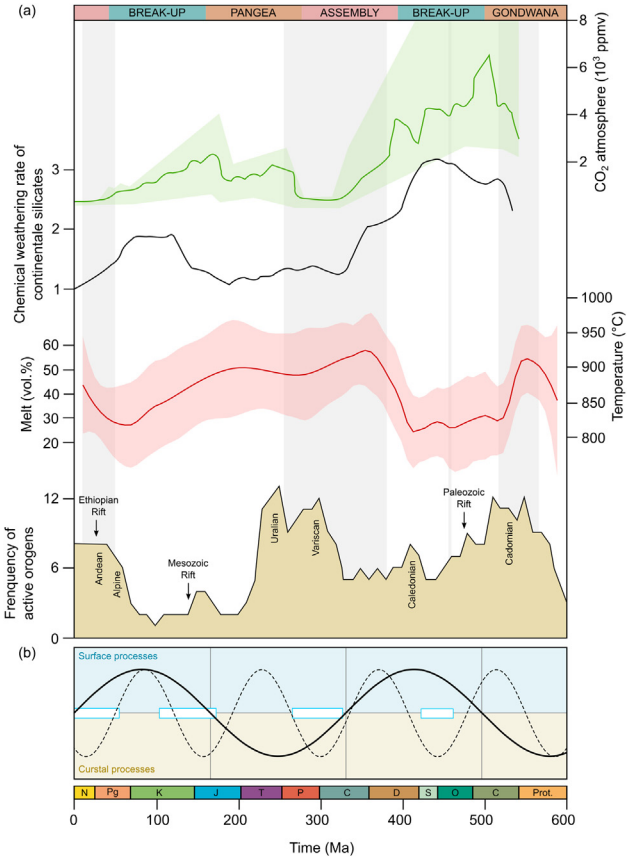

Fig. 4. Phanerozoic Wilson cycle showing the main trends in atmospheric and crustal evolution. (a) Atmospheric composition - GEOCARB III (Berner and Kothavala, 2001). Chemical weathering rate weatherability of continental silicate, calculated using the exposed land area, the average surface temperature and the atmospheric CO_2 pressure. The curve is normalised to the present day (François et al., 1993). Average metamorphic temperature in the deep crust (>850 °C and 1 GPa – Fig. 1a, with 1σ error envelope) (Brown and Johnson, 2018) and melt production equivalent from Phanerozoic shales (vol.%). Number of active orogeny after Condie et al. (2015). Rift episodes after Hunt et al. (2017); Sánchez-García et al. (2019). Vertical shaded areas highlight the presence of primary MI and FI in the geological record. (b) Cyclic volatile reservoir transfers through the Phanerozoic (plain line); cosmic cycle (dashed line) and glacial epochs (rectangle) (Berger, 2013; Brink, 2019). Crustal storage alternate with surface storage over a period of ~320 Ma.

other studies have proposed that these peaks are contemporaneous with periods of supercontinent activity and are in fact an artifact related to the preferential preservation of certain magmas during collision cycles (e.g. Hawkesworth et al., 2009, 2010; Condie et al., 2011). However, a recent statistical treatment of the geochronological archive favours the episodic production of continental material, coupled with a proportional destruction (Puetz and Condie, 2020). The second is rather unlikely, as we find nanorocks in much older terranes with a complex metamorphic history. The third option is not as far-fetched as it may sound. Nanorocks were -and still often are- found in high grade terranes already extensively investigated for decades (e.g., Kerala Khondalite belt in India, Cesare et al., 2009; Ferrero et al., 2012) or even for centuries (e.g., Bohemian Massif, Ferrero et al., 2018b; Borghini et al., 2020). This suggests that they have been previously overlooked, possibly due to their small size, coupled with the unexpected oddity of having melt inclusions, typically a feature of igneous rocks, in metamorphic rocks.,

Some studies proposed that self-sustaining subduction zones did not appear until ca. 2.0 Ga (Condie, 2018; Holder et al., 2019; Lenardic et al., 2019), others later in the Neoproterozoic (e.g. Stern, 2020). Until it did, the lack of tectonic feedback between the atmosphere and the solid Earth led to a net outgassing of water vapor, carbon dioxide and nitrogen into the primitive atmosphere and ocean (Shaw, 2008). While the loss of a significant part of the hydrogen to space led to the permanent oxidation of the Earth's surface (Catling et al., 2001; Zahnle et al., 2019), CO_2 and a part of H_2O present in the fluid envelopes were assimilated into the lithosphere through weathering processes (Bickle, 1996; West et al., 2002) and biological activity from 3.0 Ga onwards (i.e. oxygen photosynthesis – Lepot, 2020). The increase in carbon and hydrogen-saturated mineral species between 2.0 Ga and 3.0 Ga (Hazen et al., 2019) and the slow transition from stagnant-lid to mobile-lid tectonics can be then interpreted as the result of the increasing pairing between surface processes and deep Earth mechanisms (Valley et al., 2005; Sobolev and Brown, 2019).

Since 3.0 Ga critical changes in the thickness and thermal state of the crust, degree of crustal reworking and partial melting and the compositional variability of the crust (e.g. Condie, 1993; Veizer and Mackenzie, 2004; Nicoli et al., 2016; Brown and Johnson, 2018; Nicoli and Dyck, 2018; Palin et al., 2020), are thought to have led to a different, more efficient recycling method and long-term storage of volatile in the mantle through the generalisation of subduction zones (Newton, 1987; Santosh and Omori, 2008; Touret et al., 2016; Condie, 2018). Moreover, with the increase in continental volume and orogenic activity since 2.9–3.0 Ga (e.g. Dhuime et al., 2012; Condie et al., 2015), the volatile budget of the continental crust might have also grown with time (Santosh and Omori, 2008; Palya et al., 2011). Thus, the progressive storage of H, C and N in the solid Earth from 3.0 Ga onwards (e.g. Campbell and Taylor, 1983; Boerner et al., 1996; Berner and Berner, 2004; Touret et al., 2016) might have conjointly modified the physicochemical properties of Earth's solid and fluid envelopes (Korenaga, 2018). This could have launched the Earth system in a global feedback loop between deep Earth mechanisms and surface cycles (Goldblatt et al., 2009; Kerrich et al., 2006; Nisbet and Fowler, 2011).

The intrinsic link between the composition of the source (i.e. major and trace element chemistry and volatile content), the presence crustal derived magmas (e.g. Clemens et al., 2011; Nicoli et al., 2017; Villaros et al., 2009) (Fig. 2b, c) and graphite deposits (Luque et al., 2014) might suggest that some periods of Earth's history are more prone to the reworking of supracrustal lithologies than others (Campbell and Taylor, 1983). As it has been argued for the occurrence of graphite in the middle to lower crust (Oliver, 1992; Boerner et al., 1996; Wannamaker, 2000), the occurrence of primary MI and FI in the geological record could directly evidence the efficiency of the exchange and redistribution of volatiles between the surface and the crust. As most of the MI and FI are younger than 850 Ma, one could link their occurrence to the presence of well-established plate tectonic mechanisms (Brown, 2006; Brown et al., 2020; Palin et al., 2020). It is worth noting that outside the Phanerozoic and late Neoproterozoic, MI and FI in metasedimentary rocks mainly occur between 2.5 Ga and 3.0 Ga (Fig. 2b and 3a), a period interpreted by some as the transition from a stagnant-lid regime to a mobile regime (Condie, 2018 and references therein). Additionally, and despite the lack of data on inclusions between 1.6 Ga and 2.1 Ga, the relatively high abundance of S-type granites (Fig. 2c) suggests that Paleoproterozoic terrains should contain a significant amount of nanorocks and primary COH(±N) fluid inclusions. This last period corresponds to the formation of the Columbia-Nuna supercontinent, characterised by an intense orogenic activity (Condie et al., 2015), and contains the first evidence of cold, long-lasting subduction zones (e.g. Weller and St-Onge, 2017; Holder et al., 2019; Wan et al., 2020). On the other end, the lack of data for the Boring Billion (0.85-1.7 Ga) could also be explained by the presence of single lid tectonics (Stern, 2020). Little continental reconfiguration and stable atmospheric and oceanic conditions (Roberts, 2013; Condie et al., 2015) would translate into limited transfer of volatiles from the surface to the

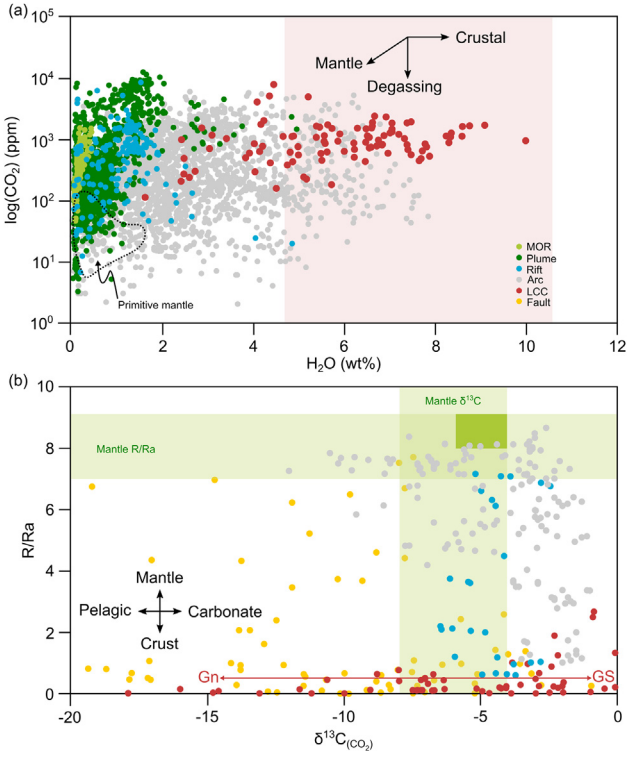

Fig. 5. Crustal input in volatile outgassing. (a) Measured volatile content (CO_2, H_2O) in melt inclusion in different geological settings (see Supplementary Data). MOR (mid-oceanic ridge) and nanorocks in the lower continental crust (LLC) represent two well-defined mantle and crustal endmembers respectively. The volatile content of plume (hot spot), arc volcanoes and continental rift might result from combination of mantle and crustal melt. The shaded area represents the range of H_2O value in nanorocks with no matching CO_2 values. Primitive mantle composition from komatiite melt inclusions. (b) Isotopic composition of volcanic and metamorphic gas (same colour code as Fig. 3a). R/Ra: $^3He/^4He$ in the sample (R), normalised to that in the atmosphere (RA = 1.38×10^{-6}), $\delta^{13}C$ reports carbon isotopes as the ratio of the heavy ^{13}C isotope relative to the lighter ^{12}C isotope relative to a standard in ‰. GS-Gn arrows indicates the range of $\delta^{13}C$ composition found in metamorphic rocks from greenschists (GS) to Gn granulite (Gn) facies conditions. *Fault* represents the outgassing of the upper to middle crust caused by earthquake.

deep crust and the mantle, as indicated by the abundance of dry magmas during this period (Ashwal, 2010; Condie et al., 2014).

Therefore, the current distribution of MI and FI in metasedimentary rocks might argue for some degree of non-unformitarianism in the evolution of plate tectonics. Further work is needed to complete the database and explore the different geodynamic scenarios mentioned above.

6. Conclusion and perspectives

The presence of preserved anatectic melt and volatile elements in inclusion in high-grade metamorphic mineral constitutes an incredible archive to investigate partial melting processes and crustal differentiation. The re-investigation of high-grade metamorphic rocks with the precise aim of finding preserved primary inclusions of deep fluids, coupled with the recent improvements in analytical techniques have showed that the amount of COH(±N) fluids in the lower crust might actually be higher than previously expected. However, while the volatile content of MI has been extensively studied in volcanic rocks, only a few studies focused on the origin and the implications of COH(±N)-fluids in MI and FI inclusions in high-grade metamorphic terranes for the evolution of geodynamic processes.

In the light of our findings, we argue that the lower crust might constitute an essential, long-term, volatile (i.e· H_2O, CO_2) storage unit, capable of influencing the composition of the surface envelopes through the mean of weathering, crustal thickening, partial melting and crustal assimilation during volcanic activity. Such hypothesis has implication beyond the scope of metamorphic petrology as it links geodynamic mechanisms to habitable surface conditions. Although most metamorphic studies focused on water and carbon dioxide, there is a still a large range of other volatile elements (e.g. S, N, Cl, F) that remain to be investigated in the context of preserved MI. Further constraints on the behaviour of volatile elements within the deep crust will be provided by future MI and FI studies in metamorphic rocks and will surely yield important new information on exchanges between reservoirs, giving greater insight into Earth's cycles.

In conclusion, that of the MI and FI in metamorphic rocks is a rich but still relatively uncharted realm. Its potential is vast but still partially untapped, as extensively discussed in the present work. In the near future, a concerted research effort should aim to find and characterise new instances of pristine inclusions in periods of the Earth's history currently underrepresented in our database, e.g. the Boring Billion. The merging of the messages of thousands of minuscule droplets of fluids trapped in the deepest roots of the continental plates will then eventually provide a truly comprehensive portrait of how the Earth's evolution proceeds through geological time.

Declaration of Competing Interest

The authors declare that they have no known competing financial interests or personal relationships that could have appeared to influence the work reported in this paper.

Acknowledgement

The authors would like to thank the editor and two anonymous reviewers for their input which helped to improve the manuscript. The present research was funded by the Alexander von Humboldt Foundation to GN and the German Federal Ministry for Education and Research and the Deutsche Forschungsgemeinschaft (Project FE 1527/2-2) to SF.

Appendix A. Supplementary data

Supplementary data to this article can be found online at https://doi.org/10.1016/j.gsf.2021.101188.

References

Acosta-Vigil, A., Buick, I., Cesare, B., London, D., Morgan, G.B., 2012. The extent of equilibration between melt and residuum during regional anatexis and its implications for differentiation of the continental crust: a study of partially melted metapelitic enclaves. J. Petrol. 53, 1319–1356.

Acosta-Vigil, A., Buick, I., Hermann, J., Cesare, B., Rubatto, D., London, D., Morgan, G. B., 2010. Mechanisms of crustal anatexis: a geochemical study of partially melted metapelitic enclaves and host dacite, SE Spain. J. Petrol 51, 785–821.

Acosta-Vigil, A., Cesare, B., London, D., VI, G.B.M., 2007. Microstructures and composition of melt inclusions in a crustal anatectic environment, represented by metapelitic enclaves within El Hoyazo dacites, SE Spain. Chem. Geol. 237, 450-465.

Acosta-Vigil, A., London, D., VI, G.B.M., Cesare, B., Buick, I., Hermann, J., Bartoli, O., 2017. Primary crustal melt compositions: Insights into the controls, mechanisms and timing of generation from kinetics experiments and melt inclusions. Lithos 286, 454-479.

Albarede, F., 2009. Volatile accretion history of the terrestrial planets and dynamic implications. Nature 461, 1227–1233.

Ashwal, L.D., 2010. The temporality of anorthosites. Canadian Minerals 48, 711-728.

Axler, J.A., Ague, J.J., 2015. Oriented multiphase needles in garnet from ultrahigh-temperature granulites, Connecticut, USA. Am. Mineral. 100, 2254–2271.

Bakker, R.J., Puskarev, E., Biryuzova, A., 2020. High temperature reduced granulite-facies nature of garnetites in the Khabarny mafic-ultramafic Massif, Southern Urals: Evidence from fluid and mineral analyses. J. Petrol. 61, egaa066.

Barich, A., Acosta-Vigil, A., Garrido, C.J., Cesare, B., Tajčmanová, L., Bartoli, O., 2014. Microstructures and petrology of melt inclusions in the anatectic sequence of Jubrique (Betic Cordillera, S Spain): Implications for crustal anatexis. Lithos 206, 303–320.

Bartoli, O., Acosta-Vigil, A., Cesare, B., Remusat, L., Gonzalez-Cano, A., Wälle, M., Tajčmanová, L., Langone, A., 2019. Geochemistry of Eocene-Early Oligocene low-temperature crustal melts from Greater Himalayan Sequence (Nepal): a nanogranitoid perspective. Contrib. Miner. Petrol. 174, 82.

Bartoli, O., Acosta-Vigil, A., Ferrero, S., Cesare, B., 2016. Granitoid magmas preserved as melt inclusions in high-grade metamorphic rocks. Am. Min. 101 (7), 1543–1559.

Bartoli, O., Cesare, B., 2020. Nanorocks: a 10–year–old story. Rendiconti Lincei. Scienze Fisiche e Naturali 31, 249–257.

Bartoli, O., Cesare, B., Poli, S., Bodnar, R.J., Acosta-Vigil, A., Frezzotti, M.L., Meli, S., 2013. Recovering the composition of melt and the fluid regime at the onset of crustal anatexis and S-type granite formation. Geology 41, 115–118.

Bartoli, O., Cesare, B., Remusat, L., Acosta-Vigil, A., Poli, S., 2014. The H_2O content of granite embryos. Earth Planet. Sci. Lett. 395, 281–290.

Baxter, E.F., Caddick, M.J., Ague, J.J., 2013. Garnet: Common mineral, uncommonly useful. Elements 9, 415–419.

Becker, J.A., Bickle, M.J., Galy, A., Holland, T.J., 2008. Himalayan metamorphic CO_2 fluxes: quantitative constraints from hydrothermal springs. Earth Planet. Sci. Lett. 265, 616–629.

Berger, A., 2013. Milankovitch and Climate: Understanding the Response to Astronomical Forcing. Springer Science & Business Media.

Berner, R.A., Berner, R.A., 2004. The Phanerozoic Carbon Cycle: CO_2 and O_2. Oxford University Press on Demand.

Berner, R.A., Kothavala, Z., 2001. GEOCARB III: a revised model of atmospheric CO_2 over Phanerozoic time. Am. J. Sci. 301, 182–204.

Black, B.A., Gibson, S.A., 2019. Deep carbon and the life cycle of large igneous provinces. Elements: An International Magazine of Mineralogy, Geochemistry, and Petrology 15(5), 319-324.

Bickle, M., 1996. Metamorphic decarbonation, silicate weathering and the long-term carbon cycle. Terra Nova 8 (3), 270–276.

Boerner, D.E., Kurtz, R.D., Craven, J.A., 1996. Electrical conductivity and Paleo-Proterozoic foredeeps. J. Geophys. Res. 101, 13775–13791.

Bolder-Schrijver, L.J.A., Kriegsmann, L.M., Touret, J.L., 2000. Primary carbonate/CO_2 inclusions in sapphirine-bearing granulites from Central Sri-Lanka. J. Metamorph. Geol. 18, 259–269.

Borghini, A., Ferrero, S., O'Brien, P.J., Laurent, O., Günter, C., Ziemann, M.A., 2020. Cryptic metasomatic agent measured in situ in Variscan mantle rocks: Melt inclusions in garnet of eclogite, Granulitgebirge, Germany. J. Metamorph. Geol. 38, 207–234.

Bradley, D.C., 2008. Passive margins through earth history. Earth Sci. Rev. 91, 1–26.

Brink, H.J., 2019. Do near-solar-system supernovae enhance volcanic activities on Earth and neighbouring planets on their paths through the spiral arms of the Milky Way, and what might be the consequences for estimations of Earth's history and predictions for its future? Int. J. Geol. 10, 563–575.

Brown, M., 2006. Duality of thermal regimes is the distinctive characteristic of plate tectonics since the Neoarchean. Geology 34, 961–964.

Brown, M., Johnson, T., 2018. Secular change in metamorphism and the onset of global plate tectonics. Am. Mineral. 103, 181–196.

Brown, M., Kirkland, C.L., Johnson, T.E., 2020. Evolution of geodynamics since the Archean: Significant change at the dawn of the Phanerozoic. Geology 48, 488–492.
Campbell, I.H., Taylor, S.R., 1983. No water, no granites-No oceans, no continents. Geophys. Res. Lett. 10, 1061–1064.
Carosi, R., Montomoli, C., Langone, A., Turina, A., Cesare, B., Iaccarino, S., Ronchi, A., 2015. Eocene partial melting recorded in peritectic garnets from kyanite-gneiss, Greater Himalayan Sequence, central Nepal. Geol. Soc. Spec. Pub. 412, 111–129.
Carvalho, B.B., Bartoli, O., Cesare, B., Tacchetto, T., Gianola, O., Ferri, F., Szabó, C., 2020. Primary CO_2-bearing fluid inclusions in granulitic garnet usually do not survive. Earth Planet. Sci. Lett. 536, 116170.
Carvalho, B.B., Bartoli, O., Ferri, F., Cesare, B., Ferrero, S., Remusat, L., Capizzi, L.S., Poli, S., 2019. Anatexis and fluid regime of the deep continental crust: new clues from melt and fluid inclusions in metapelitic migmatites from Ivrea Zone (NW Italy). J. Metamorph. Geol. 37, 951–975.
Catling, D.C., Zahnle, K.J., McKay, P.C., 2001. Biogenic methane, hydrogen escape, and the irreversible oxidation of early Earth. Science 293 (5531), 839–843.
Cesare, B., Acosta-Vigil, A., Bartoli, O., Ferrero, S., 2015. What can we learn from melt inclusions in migmatites and granulites?. Lithos 239, 186–216.
Cesare, B., Acosta-Vigil, A., Ferrero, S., Bartoli, O., 2011. Melt inclusions in migmatites and granulites. J. Virtual Explorer 38, 1441–8142.
Cesare, B., Ferrero, S., Salvioli-Mariani, E., Pedron, D., Cavallo, A., 2009. "Nanogranite" and glassy inclusions: the anatectic melt in migmatites and granulites. Geology 37, 627–630.
Cesare, B., Maineri, C., Toaldo, A.B., Pedron, D., Vigil, A.A., 2007. Immiscibility between carbonic fluids and granitic melts during crustal anatexis: a fluid and melt inclusion study in the enclaves of the Neogene Volcanic Province of SE Spain. Chem. Geol. 237, 433–449.
Chappell, B.W., Stephens, W.E., 1988. Origin of infracrustal (I-type) granite magmas. Earth Environ. Sci. Trans. 79, 71–86.
Clemens, J.D., 1990. The granulite—granite connexion. In: Vielzeuf, D., Vidal, P. (Eds.), Granulites and Crustal Evolution. NATO ASI Series (Series C: Mathematical and Physical Sciences), vol. 311. Springer, Dordrecht, pp. 25-36.
Clemens, J.D., 2003. S-type granitic magmas—petrogenetic issues, models and evidence. Earth Sci. Rev. 61, 1–18.
Clemens, J.D., Stevens, G., 2012. What controls chemical variation in granitic magmas?. Lithos 134, 317–329.
Clemens, J.D., Stevens, G., Farina, F., 2011. The enigmatic sources of I-type granites: the peritectic connexion. Lithos 126, 174–181.
Clift, P.D., Vannucchi, P., Morgan, J.P., 2009. Crustal redistribution, crust–mantle recycling and Phanerozoic evolution of the continental crust. Earth Sci. Rev. 97, 80–104.
Condie, K.C., 1993. Chemical composition and evolution of the upper continental crust: Contrasting results from surface samples and shales. Chem. Geol. 104 (1–4), 1–37.
Condie, K.C., 1998. Episodic continental growth and supercontinents: a mantle avalanche connection? Earth Planet. Sci. Lett. 163, 97–108.
Condie, K.C., 2014. How to make a continent: thirty-five years of TTG research. In: Dilek, Y., Furnes, H. (Eds.), Evolution of Archean Crust and Early Life. Modern Approaches in Solid Earth Sciences, vol. 7. Springer, Dordrecht, pp. 179-193.
Condie, K.C., 2018. A planet in transition: the onset of plate tectonics on Earth between 3 and 2 Ga?. Geosci. Front. 9, 51–60.
Condie, K.C., Bickford, M.E., Aster, R.C., Belousova, E., Scholl, D.W., 2011. Episodic zircon ages, Hf isotopic composition, and the preservation rate of continental crust. Geol. Soc. Am. Bull. 123, 951–957.
Condie, K., Pisarevsky, S.A., Korenaga, J., Gardoll, S., 2015. Is the rate of supercontinent assembly changing with time?. Precambr. Res. 259, 278–289.
Connolly, J.A.D., 2009. The geodynamic equation of state: what and how. Geochemistry, Geophys. Geosystems 10 (10) Q10014. https://doi.org/10.1029/2009GC002540.
Connolly, J.A., Trommsdorff, V., 1991. Petrogenetic grids for metacarbonate rocks: Pressure-temperature phase-diagram projection for mixed-volatile systems. Contrib. Miner. Petrol. 108, 93–105.
DePaolo, D.J., 2015. Sustainable carbon emissions: The geologic perspective. MRS Energy & Sustainability 2 (1). https://doi.org/10.1557/mre.2015.10.
Darling, R.S., 2013. Zircon-bearing, crystallized melt inclusions in peritectic garnet from the western Adirondack Mountains, New York State, USA. Geofluids 13, 453–459.
Dhuime, B., Hawkesworth, C.J., Cawood, P.A., Storey, C.D., 2012. A change in the geodynamics of continental growth 3 billion years ago. Science 335, 1334–1336.
Diener, J.F.A., Powell, R., 2012. Revised activity composition models for clinopyroxene and amphibole. J. Metamorph. Geol. 30, 131–142.
Dubacq, B., Soret, M., Jewison, E., Agard, P., 2019. Early subduction dynamics recorded by the metamorphic sole of the Mt. Albert ophiolitic complex (Gaspé, Quebec). Lithos 334, 161–179.
Eakins, B.W., Sharman, G.F., 2010. Volumes of the World's Oceans from ETOPO1. NOAA National Geophysical Data Center, Boulder, CO, p. 7.
Ferrero, S., Angel, R.J., 2018. Micropetrology: Are inclusions grains of truth?. J. Petrol. 59, 1671–1700.
Ferrero, S., Bartoli, O., Cesare, B., Salvioli-Mariani, E., Acosta-Vigil, A., Cavallo, A., Battiston, S., 2012. Microstructures of melt inclusions in anatectic metasedimentary rocks. J. Metamorph. Geol. 30, 303–322.
Ferrero, S., Bodnar, R.J., Cesare, B., Viti, C., 2011. Re-equilibration of primary fluid inclusions in peritectic garnet from metapelitic enclaves, El Hoyazo, Spain. Lithos 124, 117–131.
Ferrero, S., Braga, R., Berkesi, M., Cesare, B., Laridhi Ouazaa, N., 2014. Production of metaluminous melt during fluid-present anatexis: an example from the Maghrebian basement, La Galite Archipelago, central Mediterranean. J. Metamorph. Geol. 32, 209–225.
Ferrero, S., Godard, G., Palmeri, R., Wunder, B., Cesare, B., 2018a. Partial melting of ultramafic granulites from Dronning Maud Land, Antarctica: constraints from melt inclusions and thermodynamic modeling. Am. Min. 103, 610–622.
Ferrero, S., O'Brien, P.J., Borghini, A., Wunder, B., Wälle, M., Günter, C., Ziemann, M. A., 2018b. A treasure chest full of nanogranitoids: an archive to investigate crustal melting in the Bohemian Massif. Geol. Soc. Spec. Pub. 478, 13–38.
Ferrero, S., Wunder, B., Walczak, K., O'Brien, P.J., Ziemann, M.A., 2015. Preserved near ultrahigh-pressure melt from continental crust subducted to mantle depths. Geology 43, 447–450.
Ferrero, S., Wunder, B., Ziemann, M.A., Wälle, M., O'Brien, P.J., 2016a. Carbonatitic and granitic melts produced under conditions of primary immiscibility during anatexis in the lower crust. Earth Planet. Sci. Lett. 454, 121–131.
Ferrero, S., Ziemann, M.A., Angel, R.J., O'Brien, P.J., Wunder, B., 2016b. Kumdykolite, kokchetavite, and cristobalite crystallized in nanogranites from felsic granulites, Orlica–Snieznik Dome (Bohemian Massif): not evidence for ultrahigh-pressure conditions. Contrib. Mineral. Petrol. 171,. https://doi.org/10.1007/s00410-015-1220-x 3.
Ferri, F., Cesare, B., Bartoli, O., Ferrero, S., Palmeri, R., Remusat, L., Poli, S., 2020. Melt inclusions at MT. Edixon (Antarctica): Chemistry, petrology and implications for the evolution of the Lanterman range. Lithos 374.
Foley, S.F., Fischer, T.P., 2017. An essential role for continental rifts and lithosphere in the deep carbon cycle. Nat. Geosci. 10, 897–902.
Foster, G.L., Royer, D.L., Lunt, D.J., 2017. Future climate forcing potentially without precedent in the last 420 million years. Nat. Commun. 8, 14845.
François, L.M., Walker, J.C., Opdyke, B.N., 1993. The history of global weathering and the chemical evolution of the ocean-atmosphere system. GMS 74, 143–159.
Frost, B.R., Bucher, K., 1994. Is water responsible for geophysical anomalies in the deep continental crust? A petrological perspective. Tectonophysics 231, 293–309.
Frost, B.R., Fyfe, W.S., Tazaki, K., Chan, T., 1989. Grain-boundary graphite in rocks and implications for high electrical conductivity in the lower crust. Nature 340, 134–136.
Fuhrman, M.L., Lindsley, D.H., 1988. Ternary-feldspar modeling and thermometry. Am. Min. 73, 201–215.
Gaetani, G.A., O'Leary, J.A., Shimizu, N., Bucholz, C.E., Newville, M., 2012. Rapid reequilibration of H2O and oxygen fugacity in olivine-hosted melt inclusions. Geology 40, 915–918.
Gaillardet, J., Dupré, B., Louvat, P., Allegre, C.J., 1999. Global silicate weathering and CO_2 consumption rates deduced from the chemistry of large rivers. Chem. Geol. 159, 3–30.
Gianola, O., Bartoli, O., Ferri, F., Galli, A., Ferrero, S., Capizzi, L.S., Cesare, B., 2020. Anatectic melt inclusions in ultra high temperature granulites. J. Metamorph. Geol. 39 (3), 321–342.
Glover, P.W.J., 1996. Graphite and electrical conductivity in the lower continental crust: a review. Phys. Chem. Earth. 21, 279–287.
Goldblatt, C., Claire, M.W., Lenton, T.M., Matthews, A.J., Watson, A.J., Zahnle, K.J., 2009. Nitrogen-enhanced greenhouse warming on early Earth. Nat. Geosci. 2, 891–896.
Groppo, C., Rolfo, F., Castelli, D., Mosca, P., 2017. Metamorphic CO_2 production in collisional orogens: Petrological constraints from phase diagram modeling of Himalayan, scapolite-bearing, calc-silicate rocks in the NKC(F)MAS(T)-HC system. J. Petrol. 58, 53–83.
Guo, M., Korenaga, J., 2020. Argon constraints on the early growth of felsic continental crust. Sci. Adv. 6, eaaz6234.
Harley, S.L., 1989. The origins of granulites: a metamorphic perspective. Geol. Mag. 126, 215–247.
Hawkesworth, C., Cawood, P., Kemp, T., Storey, C., Dhuime, B., 2009. A matter of preservation. Science 323, 49–50.
Hawkesworth, C.J., Dhuime, B., Pietranik, A.B., Cawood, P.A., Kemp, A.I., Storey, C.D., 2010. The generation and evolution of the continental crust. J. Geol. Soc. 167, 229–248.
Hazen, R., Bromberg, Y., Downs, R., Eleish, A., Falkowski, P., Fox, P., Giovannelli, D., Hummer, D.R., Hystad, G., Golden, J.J., Knoll, A.H., Li, C.R., Liu, C., Moore, E.K., Morrison, S.M., Muscente, A.D., Prabhu, A., Ralph, J., Rucker, M.Y., Runyon, S.E., Warden, L.A., Zhong, H., 2019. Deep Carbon through Deep Time: Data-Driven Insights. In: Orcutt, B., Daniel, I., Dasgupta, R. (Eds.), Deep Carbon: Past to Present. Cambridge University Press, Cambridge, pp. 620–652.
Holder, R.M., Viete, D.R., Brown, M., Johnson, T.E., 2019. Metamorphism and the evolution of plate tectonics. Nature 572, 378–381.
Holland, T.J.B., Powell, R., 2011. An improved and extended internally consistent thermodynamic dataset for phases of petrological interest, involving a new equation of state for solids. J. Metamorph. Geol. 29, 333–383.
Houlton, B.Z., Morford, S.L., Dahlgren, R.A., 2018. Convergent evidence for widespread rock nitrogen sources in Earth's surface environment. Science 360, 58–62.
Huizenga, J.M., Touret, J.L., 2012. Granulites, CO_2 and graphite. Gondwana Res. 22, 799–809.
Luque, F.J., Huizenga, J.M., Crespo-Feo, E., Wada, H., Ortega, L., Barrenechea, J.F., 2014. Vein graphite deposits: geological settings, origin, and economic significance. Miner. Depos. 49, 261–277.
Hunt, J.A., Zafu, A., Mather, T.A., Pyle, D.M., Barry, P.H., 2017. Spatially variable CO_2 degassing in the Main Ethiopian Rift: implications for magma storage, volatile

transport, and rift-related emissions. Geochemistry, Geophys. Geosystems 18, 3714–3737.
Kelemen, P.B., Manning, C.E., 2015. Reevaluating carbon fluxes in subduction zones, what goes down, mostly comes up. Proc. Natl. Acad. Sci. 112, 3997–4006.
Kerrich, R., Jia, Y., Manikyamba, C., Naqvi, S.M., 2006. Secular variations of N-isotopes in terrestrial reservoirs and ore deposits. In: Kesler, S.E., Ohmoto, H. (Eds.), Evolution of Early Earth's Atmosphere, Hydrosphere, and Biosphere: Constraints from Ore Deposits. Geological Society of America, p. 81.
Kerrick, D.M., Connolly, J.A.D., 1998. Subduction of ophicarbonates and recycling of CO_2 and H_2O. Geology 26, 375–378.
Ferrero, S., Ague, J.J., O'Brien, P.J., Wunder, B., Remusat, L., Ziemann, M.A., Axler, J., 2021. High pressure, halogen-bearing melt preserved in ultra-high temperature felsic granulites of the Central Maine Terrane, Connecticut (US). American Mineralogist, in press. https://doi.org/10.2138/am-2021-7690.
Kleinefeld, B., Bakker, R.J., 2002. Fluid inclusions as microchemical systems: evidence and modelling of fluid–host interactions in plagioclase. J. Metamorph. Geol. 20, 845–858.
Klonowska, I., Janák, M., Majka, J., Petrik, I., Froitzheim, N., Gee, D.G., Sasinková, V., 2017. Microdiamond on Åreskutan confirms regional UHP metamorphism in the Seve Nappe Complex of the Scandinavian Caledonides. J. Metamorph. Geol. 35, 541–564.
Korenaga, J., 2018. Crustal evolution and mantle dynamics through Earth history. Philos. Trans. A. Math. Phys. Eng. Sci. 376, 20170408.
Kotková, J., Škoda, R., Machovič, V., 2014. Kumdykolite from the ultrahigh-pressure granulite of the Bohemian Massif. Am. Mineral. 99, 1798–1801.
Kuhn, B.K., 2004. Scapolite Stability: Phase Relations and Chemistry of Impure Metacarbonate Rocks in the Central Alps. Ph.D. thesis. ETH Zurich.
Le Breton, N., Thompson, A.B., 1988. Fluid-absent (dehydration) melting of biotite in metapelites in the early stages of crustal anatexis. Contrib. Miner. Petrol. 99, 226–237.
Lee, C.T.A., Jiang, H., Dasgupta, R., Torres, M., 2019. A Framework for Understanding Whole-Earth Carbon Cycling. In: Orcutt, B., Daniel, I., Dasgupta, R. (Eds.), Deep Carbon: Past to Present. Cambridge University Press, pp. 313–357.
Lenardic, A., Weller, M., Höink, S., Seales, J., 2019. Toward a boot strap hypothesis of plate tectonics: feedbacks between plates, the asthenosphere, and the wavelength of mantle convection. Phys. Earth Planet. Inter. 296, 106299.
Lepot, K., 2020. Signatures of early microbial life from the Archean (4 to 2.5 Ga) eon. Earth-Science Reviews 209, 103296.
Li, Z.L., Chen, H.L., Santosh, M., Yang, S.F., 2004. Discovery of ultrahigh-T spinel-garnet granulite with pure CO_2 fluid inclusions from the Altay orogenic belt, NW China. J. Zhejiang Univ. Sci. 5, 1180–1182.
Liu, Z., Bartoli, O., Tong, L., Xu, Y.G., Huang, X., 2020. Permian ultrahigh–temperature reworking in the southern Chinese Altai: evidence from petrology, P-T estimates, zircon and monazite U–Th–Pb geochronology. Gondwana Res. 78, 20–40.
Madlakana, N., Stevens, G., 2018. Plagioclase disequilibrium induced during fluid-absent biotite-breakdown melting in metapelites. J. Metamorph. Geol. 36, 1097–1116.
Mason, E., Edmonds, M., Turchyn, A.V., 2017. Remobilization of crustal carbon may dominate volcanic arc emissions. Science 357, 290–294.
Menzies, C.D., Teagle, D.A., Niedermann, S., Cox, S.C., Craw, D., Zimmer, M., Erzinger, J., 2016. The fluid budget of a continental plate boundary fault: Quantification from the Alpine Fault. New Zealand. Earth Planet. Sci. Lett. 445, 125–135.
Mposkos, E., Perraki, M., Palikari, S., 2009. Single and multiphase inclusions in metapelitic garnets of the Rhodope Metamorphic Province, NE Greece. Spectrochim. Acta Part A Mol. Biomol. Spectrosc. 73, 477–483.
Newton, R.C., 1987. Late Archaean/Early Proterozoic CO_2 streaming through the lower crust and geochemical segregation. Geophys. Res. Lett. 14, 287–290.
Newton, R.C., Smith, J.V., Windley, B.F., 1980. Carbonic metamorphism, granulites and crustal growth. Nature 288, 45–50.
Nicoli, G., 2019. Water budget and partial melting in an Archean crustal column: example from the Dharwar craton. India. Geol. Soc. Spec. Publ. 489, 115–133.
Nicoli, G., Dyck, B., 2018. Exploring the metamorphic consequences of secular change in the siliciclastic compositions of continental margins. Geosci. Front. 9, 967–975.
Nicoli, G., Moyen, J.F., Stevens, G., 2016. Diversity of burial rates in convergent settings decreased as Earth aged. Sci. Rep. 6, 26359.
Nisbet, E., Fowler, C.M.R., 2011. The evolution of the atmosphere in the Archaean and early Proterozoic. Sci. Bull. 56, 4-13.
Nicoli, G., Stevens, G., Moyen, J.F., Vezinet, A., Mayne, M., 2017. Insights into the complexity of crustal differentiation: K_2O-poor leucosomes within metasedimentary migmatites from the Southern Marginal Zone of the Limpopo Belt, South Africa. J. Metamorph. Geol. 35, 999–1022.
Oliver, J., 1992. The spots and stains of plate tectonics. Earth Sci. Rev. 32, 77–106.
O'Neill, C., Lenardic, A., Moresi, L., Torsvik, T.H., Lee, C.T., 2007. Episodic Precambrian subduction. Earth Planet. Sci. Lett. 262, 552–562.
Palin, R.M., Santosh, M., Cao, W., Li, S.S., Hernández-Uribe, D., Parsons, A., 2020. Secular change and the onset of plate tectonics on Earth. Earth Sci. Rev. 207.
Palya, A.P., Buick, I.S., Bebout, G.E., 2011. Storage and mobility of nitrogen in the continental crust: Evidence from partially melted metasedimentary rocks, Mt. Stafford. Australia. Chem. Geol. 281, 211–226.
Parisatto, M., Turina, A., Cruciani, G., Mancini, L., Peruzzo, L., Cesare, B., 2018. Three-dimensional distribution of primary melt inclusions in garnets by X-ray microtomography. Am. Mineral. 103, 911–926.
Plank, T., Manning, C.E., 2019. Subducting carbon. Nature 574, 343–352.
Pownall, J.M., Armstrong, R.A., Williams, I.S., Thirlwall, M.F., Manning, C.J., Hall, R., 2019. Miocene UHT granulites from Seram, eastern Indonesia: a geochronological–REE study of zircon, monazite and garnet. Geol. Soc. Spec. Pub. 478, 167–196.
Puetz, S.J., Condie, K.C., 2020. Applying Popperian falsifiability to geodynamic hypotheses: empirical testing of the episodic crustal/zircon production hypothesis and selective preservation hypothesis. Int. Geol. Rev., 1–31
Roberts, M.P., Finger, F., 1997. Do U-Pb zircon ages from granulites reflect peak metamorphic conditions? Geology 25, 319–322.
Roberts, N.M., 2013. The boring billion? – Lid tectonics, continental growth and environmental change associated with the Columbia supercontinent. Geosci. Front. 4, 681–691.
Roedder, E., 1984. Fluid Inclusions. De Gruyter.
Rolfo, F., Groppo, C., Mosca, P., 2017. Metamorphic CO_2 production in calc-silicate rocks from the eastern Himalaya. Ital. J. Geosci. 136, 28–38.
Ronov, A.B., Yaroshevsky, A.A., 1969. Chemical composition of the Earth's crust. GMS 13, 37–57.
Safonov, O.G., Mityaev, A.S., Yapaskurt, V.O., Belyanin, G.A., Elburg, M., Rajesh, H.M., Smit, A.C., 2020. Carbonate-silicate inclusions in garnet as evidence for a carbonate-bearing source for fluids in leucocratic granitoids associated with granulites of the Southern Marginal Zone, Limpopo Complex. South Africa. Gondwana Res. 77, 147–167.
Saitoh, Y., Tsunogae, T., 2015. Crystalized melt inclusions in mafic granulite: investigation of partial melting process based on pseudosection, in: Proc. Japan Geoscience Union Meeting 2015, Makuhari.
Salem, L.C., Edmonds, M., Corsaro, R.A., Maclennan, J., 2019. Carbon dioxide in geochemically heterogeneous melt inclusions from Mount Etna, Italy. Geochemistry. Geophys. Geosystems. 20, 3150–3169.
Sánchez-García, T., Chichorro, M., Solá, A.R., Álvaro, J.J., Díez-Montes, A., Bellido, F., Ribeiro, M.L., Quesada, C., Lopes, J.C., Dias da Silva, Í., González-Clavijo, E., Gómez Barreiro, J., López-Carmona, A., 2019. The Cambrian-Early Ordovician Rift Stage in the Gondwanan Units of the Iberian Massif. In: Quesada, C., Oliveira, J. (Eds.), The Geology of Iberia: A Geodynamic Approach. Regional Geology Reviews. Springer, Cham, pp. 27–74.
Santosh, M., Omori, S., 2008. CO_2 flushing: a plate tectonic perspective. Gondwana Res. 13, 86–102.
Santosh, M., Tsunogae, T., 2003. Extremely high density pure CO_2 fluid inclusions in a garnet granulite from southern India. J. Geol. 111, 1–16.
Sawyer, E.W., 2010. Migmatites formed by water-fluxed partial melting of a leucogranodiorite protolith: microstructures in the residual rocks and source of the fluid. Lithos 116, 273–286.
Scholl, D.W., von Huene, R., 2007. Crustal recycling at modern subduction zones applied to the past—Issues of growth and preservation of continental basement crust, mantle geochemistry, and supercontinent reconstruction. Geol. Soc. Am. Bull. 200, 9–32.
Shaw, G.H., 2008. Earth's atmosphere–Hadean to early Proterozoic. Geochemistry 68, 235–264.
Słupski, P., Ferrero, S., Walczak, K., 2018. Former melt inclusions in garnets from granulites of the Góry Sowie Block, NE Bohemian Massif. Geophys. Res. Abstracts 20.
Sobolev, A.V., Asafov, E.V., Gurenko, A.A., Arndt, N.T., Batanova, V.G., Portnyagin, M. V., Krasheninnikov, S.P., 2016. Komatiites reveal a hydrous Archaean deep-mantle reservoir. Nature 531, 628–632.
Sobolev, S.V., Brown, M., 2019. Surface erosion events controlled the evolution of plate tectonics on Earth. Nature 70, 52–57.
Spencer, C.J., Murphy, J.B., Kirkland, C.L., Liu, Y., Mitchell, R.N., 2018. A Palaeoproterozoic tectono-magmatic lull as a potential trigger for the supercontinent cycle. Nature Geosci. 11, 97–101.
Srikantappa, C., Raith, M., Touret, J.L., 1992. Synmetamorphic high-density carbonic fluids in the lower crust: evidence from the Nilgiri granulites, southern India. J. Petrol. 33, 733–760.
Stepanov, A.S., Hermann, J., Rubatto, D., Korsakov, A.V., Danyushevsky, L.V., 2016. Melting history of an ultrahigh-pressure paragneiss revealed by multiphase solid inclusions in garnet, Kokchetav massif, Kazakhstan. J. Petrol. 57, 1531–1554.
Stern, R.J., 2020. The mesoproterozoic single lid tectonic episode: prelude to plate tectonics. GSA Today 30, 4–10.
Stewart, E.M., Ague, J.J., 2018. Infiltration-driven metamorphism, New England, USA: regional CO_2 fluxes and implications for Devonian climate and extinctions. Earth Planet. Sci. Lett. 489, 123–134.
Stewart, E.M., Ague, J.J., Ferry, J.M., Schiffries, C.M., Tao, R.B., Isson, T.T., Planavsky, N. J., 2019. Carbonation and decarbonation reactions: implications for planetary habitability. Am. Min. 104, 1369–1380.
Stöckhert, B., Duyster, J., Trepmann, C., Massonne, H.J., 2001. Microdiamond daughter crystals precipitated from supercritical COH+ silicate fluids included in garnet, Erzgebirge, Germany. Geology 29, 391–394.
Tacchetto, T., Bartoli, O., Cesare, B., Berkesi, M., Aradi, L.E., Dumond, G., Szabó, C., 2019. Multiphase inclusions in peritectic garnet from granulites of the Athabasca granulite terrane (Canada): evidence of carbon recycling during Neoarchean crustal melting. Chem. Geol. 508, 197–209.
Taylor, J., Nicoli, G., Stevens, G., Frei, D., Moyen, J.F., 2014. The processes that control leucosome compositions in metasedimentary granulites: perspectives from the Southern Marginal Zone migmatites, Limpopo Belt, South Africa. J. Metamorph. Geol. 32, 713–742.
Tiwari, S.K., Rai, S.K., Bartarya, S.K., Gupta, A.K., Negi, M., 2016. Stable isotopes ($\delta^{13}C_{DIC}$, δD, $\delta^{18}O$) and geochemical characteristics of geothermal springs of

Ladakh and Himachal (India): Evidence for CO_2 discharge in northwest Himalaya. Geothermics 64, 314–330.
Touret, J.L.R., 2003. Fluids in the deep earth. J. Geochem. Explor. 78, 659–663.
Touret, J.L.R., Santosh, M., Huizenga, J.M., 2016. High-temperature granulites and supercontinents. Geosci. Front. 7, 101–113.
Valley, J.W., Lackey, J.S., Cavosie, A.J., Clechenko, C.C., Spicuzza, M.J., Basei, M.A.S., Peck, W.H., 2005. 4.4 billion years of crustal maturation: oxygen isotope ratios of magmatic zircon. Contrib. Miner. Petrol. 150, 561–580.
Veizer, J., Mackenzie, F.T., 2004. 7.15-Evolution of Sedimentary Rocks. In: Holland, H.D., Turekian, K.K. (Eds.), Treatise on Geochemistry, Vol. 7. Elsevier-Pergamon, Oxford, pp. 369–407.
Villaros, A., Stevens, G., Buick, I.S., 2009. Tracking S-type granite from source to emplacement: clues from garnet in the Cape Granite Suite. Lithos 112, 217–235.
Vry, J.K., Brown, P.E., 1991. Texturally-early fluid inclusions in garnets: evidence of the prograde metamorphic path?. Contrib. Miner. Petrol. 108, 271–282.
Wan, B., Yang, X., Tian, X., Yuan, H., Kirscher, U., Mitchell, R.N., 2020. Seismological evidence for the earliest global subduction network at 2 Ga ago. Sci. Adv. 6, eabc5491.
Wannamaker, P.E., 2000. Comment on "The petrologic case for a dry lower crust" by Bruce WD Yardley and John W. Valley. J. Geophys. Res. Solid Earth. 105, 6057–6064.
Weinberg, R.F., Hasalová, P., 2015. Water-fluxed melting of the continental crust: a review. Lithos 212, 158–188.
Weller, O.M., St-Onge, M.R., 2017. Record of modern-style plate tectonics in the Palaeoproterozoic Trans-Hudson orogen. Nat. Geosci. 10 (4), 305–311.
Werner, C., Fischer, T.P., Aiuppa, A., Edmonds, M., Cardellini, C., Carn, S., Chiodini, G., Cottrell, E., Burton, M., Shinohara, H., Allard, P., 2019. Carbon Dioxide Emissions from Subaerial Volcanic Regions. In: Orcutt, B.N., Daniel, I., Dasgupta, R. (Eds.), Deep Carbon Past to Present. Cambridge University Press.
West, A.J., Bickle, M.J., Collins, R., Brasington, J., 2002. Small-catchment perspective on Himalayan weathering fluxes. Geology 30 (4), 355–358.
White, R.W., Powell, R., Johnson, T.E., 2014. The effect of Mn on mineral stability in metapelites revisited: new aex relations for manganese-bearing minerals. J. Metamph. Geol. 32, 809–828.
Wong, K., Mason, E., Brune, S., East, M., Edmonds, M., Zahirovic, S., 2019. Deep carbon cycling over the past 200 million years: a review of fluxes in different tectonic settings. Front. Earth Sci. 7, 1–22.
Zahnle, K.J., Gacesa, M., Catling, D.C., 2019. Strange messenger: A new history of hydrogen on Earth, as told by Xenon. Geochim. Cosmochim. Acta 244, 56–85.
Zhu, Z., Campbell, I.H., Allen, C.M., Burnham, A.D., 2020. S-type granites: Their origin and distribution through time as determined from detrital zircons. Earth Planet. Sci. Lett. 536.